JOURNAL OF CATALYSIS 63, 129–137 (1980)

Kinetics of Sintering of Supported Metal Catalysts: The Mechanism of Atom Diffusion

HONG H. LEE

Department of Chemical Engineering, University of Florida, Gainesville, Florida 32611

Received August 3, 1979; revised December 12, 1979

The kinetics of sintering of supported metal catalysts is given for the rate of decay of surface area and the average particle size for the case where the prevailing mechanism of sintering is the atom diffusion. An examination of the adequacy of the central supposition of Chakraverty for typical sintering systems leads to an alternate expression for the driving force for the growth of particles and to the other results. The rate expression presented for the surface area is distinctly different from that of Ruckenstein and Pulvermacher which was obtained for the mechanism of crystallite migration. Comparisons are made between predicted values and experimental data. Results obtained indicate that the power n in the expression for the decay of surface area may not be used for the discrimination of one mechanism from the other.

INTRODUCTION

The phenomena of the growth of metal particles on a support have received considerable attention because of the importance of the surface area in the design and use of supported metal catalysts. Two mechanisms have been put forward to explain the particle growth and subsequent loss of surface area through sintering. The mechanism of atom diffusion (*1–6*) regards the difference in the interfacial energy between particles as the driving force for the particle growth. According to the mechanism, therefore, the particles redistribute themselves to minimize the overall interfacial energy of particles resulting in the growth of larger particles at the expense of smaller particles. The mechanism of crystallite migration (*7–10*) views the sintering process as a sequence of events initiated by the crystallite migration followed by collision and coalescence. The migration was considered to be due to the thermal motions of the atoms at the metal–support interface. Granquist and Buhrmam (*11–13*) examined particle size distribution curves and concluded that the two mechanisms predicted distinctly different distributions. They found that the distribution curves could be represented by the log-normal distribution of particles.

The identification of the prevailing mechanism has been based on two indirect methods and one direct method. One of the indirect methods involves the use of the shape of the particle size distribution. According to the result obtained by Granquist and Buhrman, a log-normal size distribution of particles would point to the coalescence as the prevailing mechanism. Wanke (*14*), however, found that certain initial distributions gave log-normal distribution upon sintering via interparticle transport. The other indirect method involves the use of the time dependence of the change of the surface area

$$dS/dt = -kS^n, \qquad (1)$$

where S is the exposed surface area. The atomic diffusion model predicts n values between 3 and 5 depending on the rate-limiting step whereas the crystallite migration model predicts n values ranging from <2 to >13 depending on the dependence of the diffusion coefficients and the rate constants on the crystallite size. The direct method involves the observation of actual crystallite migration.

The mechanism of atomic diffusion was

0021-9517/80/050129-09$02.00/0
Copyright © 1980 by Academic Press, Inc.
All rights of reproduction in any form reserved.

formally treated by Chakraverty (*1*) based on the classical Oswald ripening treatments of Lifschitz and Slyozov (*16*) and of Wagner (*17*). Wynblatt and Gjostein (*5, 6*) extended the results to the case of the nucleation-inhibited growth. The central supposition of the theory put forward by Chakraverty (*1*) (and subsequently used by Wynblatt and Gjostein) was that "the supersaturation is small." The supersaturation was defined as the ratio of average ad-atom concentration to the equilibrium concentration. The consequence of that central supposition is that the driving force for the particle growth can be expressed as a simple difference between the inverse of a particle size and that of the critical size, the size of the particle which neither grows nor shrinks. In this paper, we examine this central supposition and explore the consequences of not making that supposition. This leads to a conclusion that Eq. (1) does not necessarily represent the change of surface area with time when the prevailing mechanism is the atom diffusion and subsequently that the value of n may not be used to identify the prevailing mechanism. We then propose an expression for the decay of the exposed surface area for the case where the prevailing mechanism is the atom diffusion. Equation (1) was originally developed by Ruckenstein and Pulvermacher (*7*) for the mechanism of crystallite migration.

ADEQUACY OF THE SUPPOSITION OF CHAKRAVERTY

The formal treatment of Chakraverty (*1*) as rewritten by Wynblatt and Gjostein (*5*) in terms of ad-atom concentration yields the following result for the rate of growth:

$$\frac{dr}{dt} = \frac{[2\pi r a\beta' \sin\theta](2\pi D)/[\ln (L/r \sin\theta)]}{2\pi r a\beta' \sin\theta + (2\pi D)/[\ln (L/r \sin\theta)]} \times \frac{C_s^{eq}\Omega}{4\pi r^2 \alpha_1}\left\{\exp\left(\frac{2\gamma\Omega}{kTr^*}\right) - \exp\left(\frac{2\gamma\Omega}{kTr}\right)\right\}, \quad (2)$$

where

r = particle radius of curvature,
t = time,
a = interatomic spacing,
θ = wetting angle,
D = ad-atom diffusivity over the substrate ($a^2\nu_s \exp(-H_m^s/kT)$),
L = distance from the center of particle at which the ad-atom concentration reaches its far-field concentration,
C_s^{eq} = concentration of ad-atoms on the substrate,
Ω = volume of an ad-atom,
α_1 = volume shape factor,
γ = surface energy of the particle,
k = Boltzmann constant,
T = absolute temperature,
r* = size of the particle which neither shrinks nor grows in the particle size distribution, critical size,
β' = $\nu_m \exp(-H_s^s/kT)$,
ν_s = vibrational frequency of an ad-atom on the substrate
H_m^s = migration energy of an ad-atom on the substrate.

The central supposition of Chakraverty (*1*) essentially enables one to rewrite the quantity inside the bracket of Eq. (2) as

$$\exp\left(\frac{2\gamma\Omega}{kTr^*}\right) - \exp\left(\frac{2\gamma\Omega}{kTr}\right) \approx \frac{2\gamma\Omega}{kT}\left(\frac{1}{r^*} - \frac{1}{r}\right). \quad (3)$$

We wish to examine the adequacy of this supposition. The critical size r^* can be related to the mean size $\bar{r}$ (*17, 18*) by

$$\bar{r} = br^*, \quad (4)$$

where b is a constant close to unity. Since the typical particle size distributions are such that the majority of particles belongs to the size range of ($0.5\bar{r} < r < 2\bar{r}$), we compare the magnitude of the left-hand side (LHS) of Eq. (3) with that of the right-hand

side (RHS) for various values of $(2\gamma\Omega/(kTr^*))$ as a function of r in the size range of $(0.5r^* < r < 2r^*)$. For this, we define the following quantities:

$$\rho \equiv \frac{r}{r^*(t)} \tag{5}$$

$$\epsilon \equiv \frac{2\gamma\Omega}{kTr^*}. \tag{6}$$

If we use the definitions, we can rewrite Eq. (3) as

$$\exp(\epsilon) - \exp(\epsilon/\rho) \approx \epsilon(1 - 1/\rho). \tag{7}$$

Computational results for the magnitudes are shown in Figs. 1 and 2. The difference given by Eq. (7) is a measure of the magnitude of the concentration difference (refer to Eq. (2)), which is the driving force for the growth or shrinkage of particles. Results in Fig. 1 show that this magnitude is almost the same for the scale chosen when $\epsilon = 0.1$ whether the magnitude is calculated from the RHS or the LHS of Eq. (7). Therefore, the supposition of Chakraverty is adequate as long as the dimensionless surface energy for the critical size, ϵ, is less than 0.1. However, the supposition is not adequate when ϵ becomes larger than, say, 0.2 as shown in Fig. 1 for $\epsilon = 0.5$. The dashed line represents the magnitude calculated from the RHS of Eq. (7) and the solid line from the LHS of Eq. (7). Even though not shown, the error in using the RHS of Eq. (7) for the calculation of the magnitude can be as high as 25% even for $\epsilon = 0.2$.

The importance of this fact lies in the fact that for some of the supported metal catalysts of interest, the value of ϵ is typically in the range of 0.1 to 1 under typical sintering conditions. The sintering study of Pt crystallites on alumina by Wynblatt (*6*), for instance, was in the ϵ range of 0.3 to 0.8 at 1000°K. The sintering study of Pt crystallites on amorphous S_iO_2 by Chen and Schmidt, for another, was in the range of 0.35 to 0.75 at 1000°K. The critical size was of the order of 5 to 15 nm. Recognizing this inadequacy of Chakraverty's supposition for the typical sintering problems, we set out to develop an expression for the con-

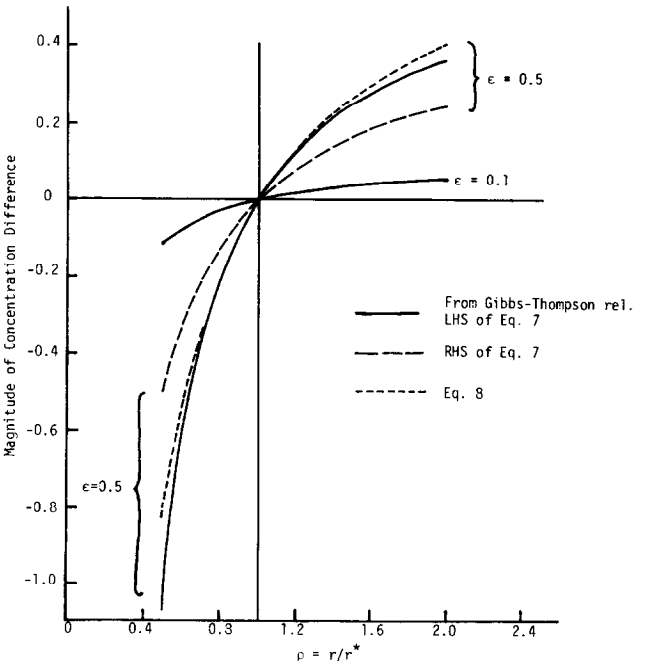

FIG. 1. A measure of magnitude of concentration difference determined from different relationships, $\epsilon = 0.5$ and $\epsilon = 0.1$.

centration difference which would be good up to ϵ of 1. To obtain this expression, we rewrite the quantity inside the bracket of Eq. (2) as

$$\exp\left(\frac{2\gamma\Omega}{kTr^*}\right) - \exp\left(\frac{2\gamma\Omega}{kTr}\right) = \exp\left(\frac{2\gamma\Omega}{kTr^*}\right)\left\{1 - \exp\left[\frac{2\gamma\Omega}{kTr}\left(1 - \frac{r}{r^*}\right)\right]\right\}$$
$$\approx -\left[\exp\left(\frac{2\gamma\Omega}{kTr^*}\right)\right]\left\{\frac{2\gamma\Omega}{kTr}\left(1 - \frac{r}{r^*}\right)\right\} = -\left(\frac{1-\rho}{\rho}\right)\epsilon\exp(\epsilon), \quad (8)$$

where the exponential term inside the bracket of the second expression was expanded in Taylor series for the approximation and the definitions of ρ and ϵ were used for the last expression. The magnitude of concentration difference given by Eq. (8) is shown in Figs. 1 and 2 as the dotted lines. The results show that Eq. (8) is adequate up to ϵ of 0.8 and possibly up to 1 for the range of size shown.

RATE OF DECAY OF SURFACE AREA

We now utilize the result obtained for the concentration difference [Eq. (8)] in Eq. (2) for the rate of growth:

$$\frac{dr}{dt} = -\frac{A_D}{r^3}\left(1 - \frac{r}{r^*}\right)\exp\left(\frac{2\gamma\Omega}{r^*kT}\right), \quad (9)$$

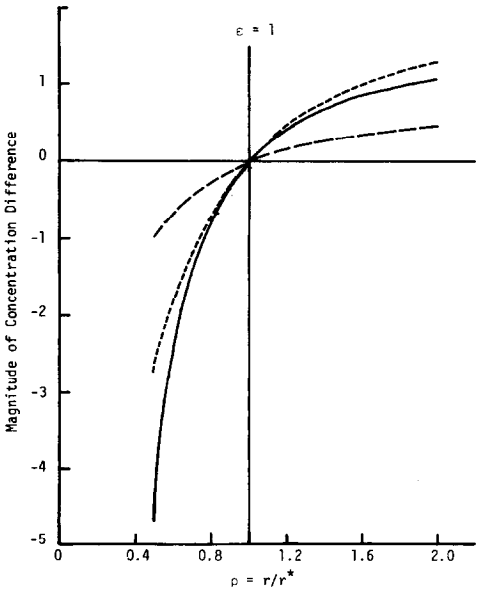

FIG. 2. A measure of magnitude of concentration difference determined from different relationship, ϵ = 1.

where

$$A_D \equiv \frac{D\gamma\Omega^2 C_s^{eq}}{\alpha_1 kT \ln[L/r \sin\theta]}. \quad (9a)$$

In accordance with the argument of Wynblatt and Gjostein (*5*), the resistance across the edge of the particle was neglected in rewriting Eq. (2). It is seen that Eq. (9) reduces to the result of Wynblatt and Gjostein when the value of ϵ is small.

If we let $f(r, t)$ be the number of particles in the size range between r and $r + dr$, the number balance (*16*) can be written as

$$\frac{\partial f}{\partial t} + \frac{\partial}{\partial r}\left(f\frac{dr}{dt}\right) = 0. \quad (10)$$

In terms of the dimensionless size ρ defined by Eq. (5), the number balance can be rewritten as

$$\frac{\partial f_s}{\partial t} + \frac{\partial}{\partial \rho}\left(f_s\frac{d\rho}{dt}\right) = 0, \quad (11)$$

where $f_s(\rho, t)$ is the number of particles in the dimensionless size range between ρ and $\rho + d\rho$. Utilizing the definition of ρ [Eq. (5)], the growth rate in terms of the dimensionless size can be obtained from Eq. (9):

$$\frac{d\rho}{dt} = -\rho\frac{\dot{r}^*}{r^*} - \frac{A_D(1-\rho)}{\rho^3(r^*)^4}\exp\left(\frac{\beta}{r^*}\right), \quad (12)$$

where

$$\beta = \frac{2\gamma\Omega}{kT}. \quad (12a)$$

The total number of particles $N(t)$, the surface area $S(t)$, and the total volume of particles ϕ which is conserved are given by

$$N(t) = \int_0^\infty f_s d\rho, \quad (13)$$

$$S(t) = \int_0^\infty (\alpha_2 r^* \rho)^2 f_s d\rho, \quad (14)$$

$$\phi = \text{const} = \int_0^\infty (\alpha_1 r^* \rho)^3 f_s d\rho, \quad (15)$$

where α_2 is the shape factor for the surface area. It is noted that the particle of the dimensionless size ρ has the surface area associated with it of $(\alpha_2 r^* \rho)^2$. As was done by Chakraverty (*1*) and Ruckenstein and Pulvermacher (*7*), we assume that the distribution function f_s is separable such that

$$f_s(\rho, t) = h(t)\, g(\rho). \quad (16)$$

Utilizing Eq. (16) in Eqs. (13) through (15), we obtain

$$h(t) = N/B_1, \quad (17)$$

$$r^*(t) = \left(\frac{B_1\phi}{NB_2}\right)^{1/3}, \quad (18)$$

$$S(t) = \frac{B_3}{B_1} N(r^*)^2, \quad (19)$$

where

$$B_1 = \int_0^\infty g(\rho)d\rho, \quad (20)$$

$$B_2 = \int_0^\infty (\alpha_1\rho)^3 g(\rho)d\rho, \quad (21)$$

$$B_3 = \int_0^\infty (\alpha_2\rho)^2 g(\rho)d\rho. \quad (22)$$

If we integrate Eq. (11) with respect to ρ from zero to infinity, we obtain

$$\frac{dN}{dt} = h(t)\left\{A_1 \frac{\dot{r}^*}{r^*} + A_2 A_D \frac{\exp(\beta/r^*)}{(r^*)^4}\right\}, \quad (23)$$

where

$$A_1 = \int_0^\infty \frac{\partial}{\partial\rho}[\rho g(\rho)]d\rho,$$

$$A_2 = \int_0^\infty \frac{\partial}{\partial\rho}\left[\frac{1-\rho}{\rho^3} g(\rho)\right] d\rho. \quad (24)$$

From Eq. (18), we obtain

$$\frac{\dot{r}^*}{r^*} = -\tfrac{1}{3} N^{-1}\dot{N}. \quad (25)$$

We relate the surface area to the total number of particles using Eqs. (18) and (19) to obtain

$$S = \frac{B_3}{B_1}\left(\frac{B_1\phi}{B_2}\right)^{2/3} N^{1/3}. \quad (26)$$

The relationship between the surface area and the critical size can be obtained by using Eq. (18) in (26):

$$r^* = \left(\frac{B_3\phi}{B_2}\right)\left(\frac{1}{S}\right). \quad (27)$$

If we utilize Eqs. (17), (25), and (27) in Eq. (23), we obtain

$$\frac{dN}{dt} = \frac{A_2 A_D}{(1 + A_1/3B_1)B_1}\left(\frac{B_2}{B_3\phi}\right)^4 \times NS^4 \exp\left[\frac{B_2\beta}{B_3\phi} S\right]. \quad (28)$$

Finally, we use Eq. (26) in (28) to obtain

$$\frac{ds}{dt} = -KS^5 \exp(mS), \quad (29)$$

where

$$K(T) = \left(\frac{A_2 A_D}{3B_1 + A_1}\right) \times \left(\frac{B_2}{B_3\phi}\right)^4 \left(\frac{B_1}{B_3}\right)^2 \left(\frac{B_2}{B_1\phi}\right)^{4/3}, \quad (30)$$

$$m(T) = \frac{\beta B_2}{B_3\phi}. \quad (31)$$

Consider the temperature dependence of the quantities K and m. The terms A_i and B_i in the expression for K are integrals of $g(\rho)$. While a full solution of the size distribution is not attempted here, it is nevertheless possible to ascertain the temperature dependence of $g(\rho)$ by examining a solution for $g(\rho)$ obtained by Chakraverty (*1*), which corresponds to our case when ϵ [Eq. (12a)] is much less than unity. A solution for $g(\rho)$ obtained by Chakraverty [Eq. (25) in Ref. (*1*)] does not contain any temperature-dependent terms. This leaves A_D as the sole term in the expression for K that is dependent on temperature. Utilizing Eq. (9a) for A_D, then, the temperature dependence of K can be expressed as

$$K = k_0 T^{-1} \exp(-E_a/kT), \quad (32)$$

where

$$k_0 = \frac{\bar{k}a^2\nu_s\gamma\Omega^2}{k\alpha_1 l\ln[L/r\sin\phi]}\left(\frac{A_2}{3B_1 + A_1}\right) \times \left(\frac{B_2}{B_3\phi}\right)^4\left(\frac{B_1}{B_3}\right)\left(\frac{B_2}{B_1\phi}\right)^{2/3}, \quad (32a)$$

$$E_a = H_e + H_m{}^s. \quad (32b)$$

The temperature dependence of the ad-atom concentration on the substrate $C_e{}^{eq}$ which would be in equilibrium with an infinite-sized particle was expressed in Eq. (32a) as

$$C_s{}^{eq} = \bar{k}\exp(-H_e/kT),$$

where the free energy in the exponential was approximated by the enthalpy H_e. The quantity $H_m{}^s$ in Eq. (32b) is the activation energy for the migration of an ad-atom. We note that the term ϕ in Eq. (32a) is the total metal volume [Eq. (15)], which would be conserved and therefore constant so long as the metal density does not change significantly with temperature in the temperature range of typical sintering experiments. Therefore, the term ϕ can be considered relatively constant for a given catalyst system. Applying the same argument for ϕ to Eq. (31), the temperature dependence of m is due to β which is inversely proportional to temperature [Eq. (12a)]. For a small temperature range, therefore, m may be considered constant.

Similar derivations lead to the following expression for the case where the interparticle transport takes place through the vapor phase:

$$\frac{dS}{dt} = -K'S^3\exp(mS). \quad (33)$$

The main conclusion of this section is that the rate of decay of the exposed surface area of metal is given by an equation of the form

$$\frac{dS}{dt} = KS^n\exp(mS) \quad (34)$$

$n = 5$ for substrate-diffusion transport

$n = 3$ for vapor-phase transport

when the prevailing mechanism for sintering is the atomic diffusion. This result contrasts the equation developed by Ruckenstein and Pulvermacher (*7*) for the sintering mechanism of the crystallite migration:

$$\frac{dS}{dt} = -K_c S^{n_c}. \quad (35)$$

It is noted that the value of n is not arbitrary but rather fixed as shown in Eq. (34).

AVERAGE PARTICLE SIZE

Before we proceed to derive an expression for the change of average crystallite size with time, we apply Eq. (34) to the data obtained by Richardson and Cump (*19*) on nickel catalyst on silica sintered in helium. They obtained crystallite size distributions using a magnetic granulometry method (*20*). Illustration of the use of Eq. (34) is one of the purposes of considering the data. The other is to make a point that the value of n in Eq. (1) may not be used for the purpose of determining which mechanism dominates the sintering process. If the crystallite growth were due to the atom migration, the substrate-diffusion rather than the vapor-phase transport would dominate the transport process at the temperature of sintering (<600°C). We write Eq. (34) as follows:

$$\frac{dS}{dt} = -KS^5\exp(m'S/S_0), \quad (36)$$

where S_0 is the initial exposed surface area and $m' = mS_0$. For the analysis of the data, we rewrite Eq. (36) as

$$\int_S^{S_0}\frac{dS}{S^5\exp(m'(S/S_0))} = Kt. \quad (37)$$

For the right value of m', then, a plot of the left-hand side of Eq. (37) against time should yield a straight line through the origin with the slope of K. If we use the value of m' at the midpoint of the experimental temperature range, say, 800°K for the sintering temperature range used by Richardson and Crump (*19*), we may neglect the temperature dependence of m' and the value of the

chosen m' could be considered constant for different sintering temperatures. Based on the sintering data of Richardson and Crump (Fig. 4 of their article) and Eq. (37), we determined K values at different sintering temperatures with the chosen m' value of 3. The corresponding Arrhenius plot is shown in Fig. 3. The apparent activation energy was determined from the plot to be 154 (kJ/mole). Because of the high apparent activation energy, the effect of T^{-1} in Eq. (32) is negligible. Using the K values given by the straight line in Fig. 3, the normalized surface area (S/S_0) were calculated and compared with their experimental data. The goodness of the fit was comparable to that of the fit obtained by Richardson and Crump. They used Eq. (35) for their fit. While only the direct observation, as was done by Baker *et al.* (*22*), can conclusively tell whether the dominating mechanism is the crystallite migration or the atom diffusion, the result of the present analysis can be used if so desired to argue for the mechanism of atom diffusion. It should be recognized, however, that this example was treated to show that the value of n may not be used for the purpose of discriminating one mechanism from the other and not to argue for or against the mechanism of crystallite migration. The dominating mechanism for the sintering studied by Richardson and Crump may indeed be that of crystallite migration.

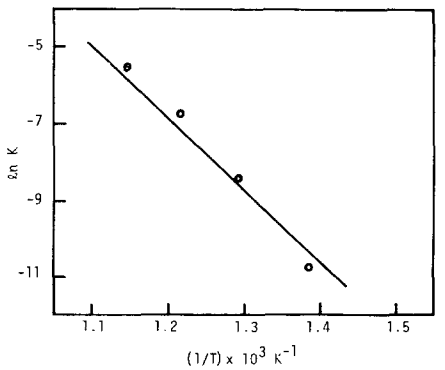

FIG. 3. An Arrhenius plot for the sintering data of Ni (experimental data from Richardson and Crump (*19*)).

The dimensionless surface energy for the critical size ϵ [Eq. (12a)] for the nickel system being considered is approximately 1.5 at 873°K and 1.9 at 773°K if we use the surface energy of Ni at 1470°C (*21*), which is 1735 erg/cm². In view of the conclusion made in the previous section, one might question the applicability of Eq. (36) to the nickel sintering being considered. However, the size distributions for this system are relatively sharp such that the majority of the particles belongs to the dimensionless size range of $0.9 < \rho\ (=r/r^*) < 1.1$ at 773°K and $0.8 < \rho < 1.5$ at 873°K [Fig. 2 and 3 of Ref. (*19*)]. If we refer to Fig. 1 or 2, we see that the error becomes small as ρ approaches unity. Therefore, Eq. (36) can be applied to this system.

The growth rate of the critical size can be obtained by substituting Eq. (27) into Eq. (29) for the case of substrate-diffusion transport:

$$\frac{dr^*}{dt} = \frac{K_r}{(r^*)^3} \exp(\beta/r^*), \tag{38}$$

where

$$K_r = K(B_3\phi/B_2)^4. \tag{38a}$$

Since the average particle size is related to the critical size by Eq. (4) [$b = 1.03$ for the substrate-diffusion transport (*18*) and $b = 8/9$ for the vapor-phase transport (*17*)], we have for the average particle size

$$\frac{d\bar{r}}{dt} = \frac{\bar{K}}{(4\bar{r})^3} \exp\left(\frac{b\beta}{\bar{r}}\right), \tag{39}$$

where $\bar{K} = Krb^4$. We apply Eq. (39) to the growth vs time data obtained by Chen and Schmidt (*15*). In particular, we apply the equation to the data given in Fig. 7 of their article for the sintering of Pt crystallite on amorphous SiO_2. The value of ϵ at 650°C is around 0.5 [$\gamma = 2100$ erg/cm² (*5*)]. The value of β is 4.88 nm. Therefore, we have from Eq. (39).

$$\frac{d\bar{r}}{dt} = \frac{\bar{K}}{(\bar{r})^3} \exp\left(\frac{5.02}{\bar{r}}\right) \qquad (\bar{r} \text{ in nm}). \tag{40}$$

We fit the data of Chen and Schmidt (*15*) using Eq. (40) by choosing $\bar{K}$ values and the results are given in Fig. 4 along with the experimental data. The value of $\bar{K}$ chosen for the sintering in N_2 is 650 $(nm)^4/hr$ and in air 4000 $(nm)^4/hr$. It is seen that Eq. (40) represents the experimental data fairly well. Chen and Schmidt used an equation of the form of Eq. (1) and found the n value to be 6 for the sintering in air and 10 in N_2.

We also attempted to apply Eq. (39) to the sintering data obtained by Wynblatt (*6*) for the sintering of Pt crystallite on alumina. They found that their results in O_2 could be well represented by the nucleation-inhibited atomic diffusion model with PtO_2 as the transport species. Our attempts revealed that their data could not be well represented by Eq. (39). This fact seems to render credence to the use of the nucleation-inhibited growth model for their sintering system.

CONCLUSION

The rate of decay of the exposed surface area of the supported metal catalysts, when the mechanism of sintering is the atom diffusion, is given by an equation of the form

$$\frac{dS}{dt} = -KS^n \exp(mS),$$

where n is 5 for the case of substrate-diffusion transport and 3 for that of vapor-phase transport. In contrast, Ruckenstein and Pulvermacher (*7*) obtained an equation of the form

$$\frac{dS}{dt} = -K_c S^{n_c}$$

for the mechanism of crystallite migration. The results presented here apply up to the ϵ value [Eq. (6)] of unity for typical size distributions. For sharper size distributions, they apply to higher values of ϵ. The majority of sintering systems of interest belongs to this range of ϵ for typical sintering conditions. The temperature dependence of the rate constant K is mainly due to the temperature dependence of the diffusivity and the equilibrium concentration of an infinite-sized particle. The quantity m is a weak function of temperature and may be taken constant for a small temperature range. Results obtained indicate that the value of n in Eq. (1) may not be used for the purpose of discriminating one mechanism from the other.

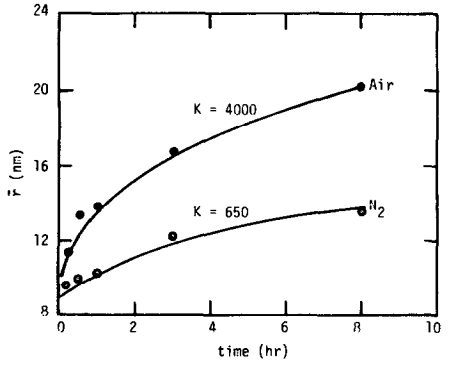

FIG. 4. Growth of average particle size (data from Chen and Schmidt (*15*)).

REFERENCES

1. Chakraverty, B. K., *J. Phys. Chem. Solids* **28**, 2401 (1967).
2. Flynn, P. C., and Wanke, S. E., *J. Catal.* **34**, 390 (1974).
3. Flynn, P. C., and Wanke, S. E., *J. Catal.* **34**, 400 (1974).
4. Wynblatt, P., and Gjostein, N. A., *Progr. Solid State Chem.* **9**, 21 (1975).
5. Wynblatt, P., and Gjostein, N. A., *Acta Met.* **24**, 1165 (1976).
6. Wynblatt, P., *Acta Met.* **24**, 1175 (1976).
7. Ruckenstein, E., and Pulvermacher, B., *AIChE J.* **19**, 356 (1973).
8. Ruckenstein, E., and Pulvermacher, B., *J. Catal.* **29**, 224 (1973).
9. Pulvermacher, B., and Ruckenstein, E., *J. Catal.* **35**, 115 (1974).
10. Ruckenstein, E., and Dadyburjar, D. B., *J. Catal.*, **48**, 73 (1977).
11. Granquist, C. G., and Buhrman, R. A., *J. Appl. Phys.*, **27**, 693 (1975).
12. Granquist, C. G., and Buhrman, R. A., *J. Appl. Phys.*, **47**, 2200 (1976).
13. Granquist, C. G., and Buhrman, R. A., *J. Catal.*, **46**, 238 (1977).
14. Wanke, S. E., *J. Catal.* **46**, 234 (1977).
15. Chen, M., and Schmidt, L. D., *J. Catal.* **55**, 348 (1978).

16. Lifschitz, I. M., and Slozov, V. V., *J. Phys. Chem. Solids* **19,** 35 (1961).

17. Wagner, C., *Z. Electrochem.* **65,** 581 (1961).

18. Kirchner, H. O. K., *Met. Trans.* **2,** 2861 (1971).

19. Richardson, J. T., and Crump, J. G., *J. Catal.* **57,** 417 (1979).

20. Richardson, J. T., and Desai, P., *J. Catal.* **42,** 294 (1976).

21. Bikerman, J. J., "Surface Chemistry: Theory and Applications," p. 34. Academic Press, New York, 1958.

22. Baker, R. T. K., Thomas, C., and Thomas, R. B., *J. Catal.* **38,** 510 (1975).